energies

MDPI

Article

Low-Carbon Scheduling of Integrated Electricity and Gas Distribution System Considering V2G

Yicheng Li, Lixiong Xu *, Xiangmei Lv and Yiran Xiao

College of Electrical Engineering, Sichuan University, Chengdu 610017, China
* Correspondence: xulixiong@scu.edu.cn

Abstract: With the development of EVs (Electric Vehicles) and the rapidly developing policies on low carbon and environmental protection, electric power systems and natural gas systems become increasingly larger. Under these circumstances, the V2G (Vehicle-to-grid) and the coordinated operation of an integrated electricity–gas distribution system (IEGDS), considering CO_2 emissions, can play a part together in the process of energy conservation. Firstly, the V2G model is discussed; this paper presents the cost differences between out-of-order and order for the car. Secondly, the IEGDS model presents coupling constraints of gas turbines and power-to-gas. Lastly, carbon emission is considered in this paper; a carbon capture plant (CCP) captures the CO_2 burning by fossil fuel in the power generation process and stores it in a carbon storage tank. This paper also considers trading with the carbon market via a carbon storage warehouse. With the cooperation of various components, a comprehensive model considers the use of V2G to store power in the IEGDS system, with consideration of the carbon trade. Numerical experiments validate the effectiveness of the combination between V2G and IEGDS, considering carbon emissions and carbon trading.

Keywords: V2G; power system; evaluation methods; natural gas system; integrated electricity–gas system; carbon emission; carbon trade

Citation: Li, Y.; Xu, L.; Lv, X.; Xiao, Y. Low-Carbon Scheduling of Integrated Electricity and Gas Distribution System Considering V2G. *Energies* **2022**, *15*, 9524. https://doi.org/10.3390/en15249524

Academic Editor: Dimitrios Katsaprakakis

Received: 10 October 2022
Accepted: 1 November 2022
Published: 15 December 2022

1. Introduction

Nowadays, with the development of the economy, the demand for energy is increasing at a high speed. Conventional fossil energy contributes to carbon dioxide emissions which can cause global warming. According to the World Meteorological Organization (WMO) report, compared with the averages, the average temperatures in 1991–2000, 2001–2007 and 2008–2017 were 0.21 °C, 0.44 °C and 0.51 °C higher [1]. To curb this trend, we should increase the development of green sustainable energy. Wind power and photovoltaics (PV) generation as high-quality clean energy have received full attention [2]. However, in the process of wind power generation and photovoltaics development, many problems slowly appear, among which the problem of wind and PV power absorption has become the most important, and the phenomenon of wind and PV curtailment is common in some places where wind and PV energy is abundant. Because of the strong fluctuation of wind and PV power optoelectronics and the limited regulation ability of traditional energy power generation, it cannot absorb wind and PV power optoelectronics on a large scale, which hinders the progress and development of wind power and PV generation [3]. However, more and more countries in the world are vigorously developing PV and wind power to reduce carbon emissions [4]. At the same time, China has asked for carbon neutralization and an emission peak, striving to reach the emission peak by 2030 and carbon neutralization by 2060 [5]. In this context, in order to further improve the absorption capacity of wind and PV energy and low-carbon economic scheduling, this paper will study renewable energy absorption and low-carbon economic scheduling in the context of a variety of energy sources.

Due to good environmental and economic benefits, electric vehicles have been fully developed, and the energy battery of an electric vehicle, as an energy storage resource,

can actively participate in the active distribution network [6]. Under the background of distributed energy, the orderly charge and discharge model of electric vehicle in the active distribution network is established. In reference [3,7], an orderly charge–discharge model for electric vehicles with wind power and photovoltaics access is established. It can be seen that only the access of electric vehicles, a single variable, is considered in some literatures, and the ability to absorb it is also relatively limited.

This paper further explores the above phenomena. It is found that power-to-gas (P2G) is a great help to absorption. In reference [8], the power consumption of P2G equipment is provided by the wind curtailment of wind power equipment, and a model of directly absorbing wind curtailment is given. In this case, power–gas interconnection is needed to ensure absorption. References [9,10] establishes the demand response of power-gas interconnection to promote the coordination of the power grid and gas network. Reference [11] states that the gas turbine is expected to replace some traditional generators and carbon emissions are lower in this process. In reference [12], the model of an integrated electricity–gas distribution system (IEGDS) is given, and the nonlinear natural gas power flow containing a natural gas system in a gas–electric interconnection system. There are two ways to deal with nonlinear natural gas power flow in gas–electric interconnection system. ① Convert the original problem to a mixed integer linear programming model by linearization. ② Convert the original problem to a mixed integer second-order conical (SOC) solution using cone optimization. In reference [13], the famous Weymouth steady-state natural gas power flow equation is linearized by a piecewise linearization method. In reference [14], the power flow equation of the power system and natural gas system is treated by a SOC programming method, and the power flow equation of gas network is relaxed by SOC in reference [15], which is transformed into a mixed integer second-order cone programming model. In references [16,17], a model of gas distribution with renewable energy is given. Reference [18] establishes a model of gas distribution considering V2G.

In order to operate the low-carbon economy of the whole system, low-carbon technology and a reasonable market mechanism are needed to intervene. For the power grid, in addition to the increased use of renewable energy, carbon dioxide emission absorption from the power grid is one of the options, CCS (carbon capture and storage) technology plays an important role in carbon dioxide emission reduction, reference [19] proposed a technical model for carbon dioxide capture and storage, reference [20] gave the CCS model in the case of V2G, reference [21] considered the income in the energy market and the carbon market when an electric vehicle was connected in an orderly manner. In order to reduce the cost, reference [22] gave a model on the condition that the main power grid includes wind power plants. For the model of carbon collection, the CCS model with the participation of optoelectronics is given in reference [23]. In addition to the participation of the main power grid, because of IEGDS, the emergence of a gas network also needs to introduce CCP technology. The model of using CCP technology while including P2G equipment is given in reference [21]. The cost calculation of combining carbon capture technology with IEGDS in the case of V2G is given in reference [22]. To reduce the cost of the carbon emission process, carbon trading is included in reference [24]. A model of carbon trading with integrated energy systems is given in reference [25]. A model of carbon trading with renewable energy is given in reference [26], reference [27] gave a carbon trading model with V2G. Reference [28] gave a carbon trading model considering P2G devices.

On the basis of the above study, in order to complete peak shaving and valley filling, control the cost of the main grid and reduce the carbon emission of whole system, the low carbon dispatching problem of an integrated electricity and natural gas distribution system considering V2G is studied in this paper.

(1) This paper introduces V2G to consume renewable energy as well as suppress the peak-to-valley difference of the net load of the grid, and give full play to the advantages of the orderly access of electric vehicles to the grid.
(2) After the access of P2G devices, the renewable energy consumption capacity of the system is further improved and the cost is controlled Secondly, after the P2G devices

are connected, the renewable energy consumption capacity of the system is further improved and the cost is controlled.

(3) Carbon trading is considered in the whole system to meet the requirements of low-carbon emissions, which also allows the cost of enterprises to be reduced.

(4) The low-carbon dispatch model of the integrated power and natural gas distribution system considering V2G is obtained, and the innovative combination of the above three types of grid dispatch schemes is used to obtain the positive effect of this paper on the low-carbon dispatch of the integrated power and natural gas distribution system considering V2G through simulation.

2. The Coordinated Operation of an Integrated Electricity–Gas Distribution System Considering Carbon Trading

The IEGDS system considers the electrical system, the natural gas network and the electric–gas interconnected system. In this paper, wind farms and photovoltaic power generation are added to the grid. In addition, the carbon emission operation model of the whole system is also considered. In Figure 1, the distribution network receives power mainly from gas turbines and substations, while the rest is supplied by wind farms and photovoltaic power generation. Because of the possibility of wind abandonment and light abandonment due to the incorporation of renewable energy units, we have integrated electric vehicles and P2G systems (which convert hydrogen and carbon dioxide from water and electrolysis into methane) throughout the system to convert excess energy into the energy battery of the electric vehicle and the chemical energy contained in the natural gas system. In order to further "peak shaving and valley filling", the system will ensure the power supply of the main grid through the access of electric vehicles and the starting of gas turbines when more power is needed. In this process, we will treat electric vehicle clusters as distributed energy storage units. Carbon emissions generated during the entire system operation will be: collected by CCP units, partially involved in the operation of P2G devices, partially transported to nearby carbon storage warehouses, participating in the local carbon trading market.

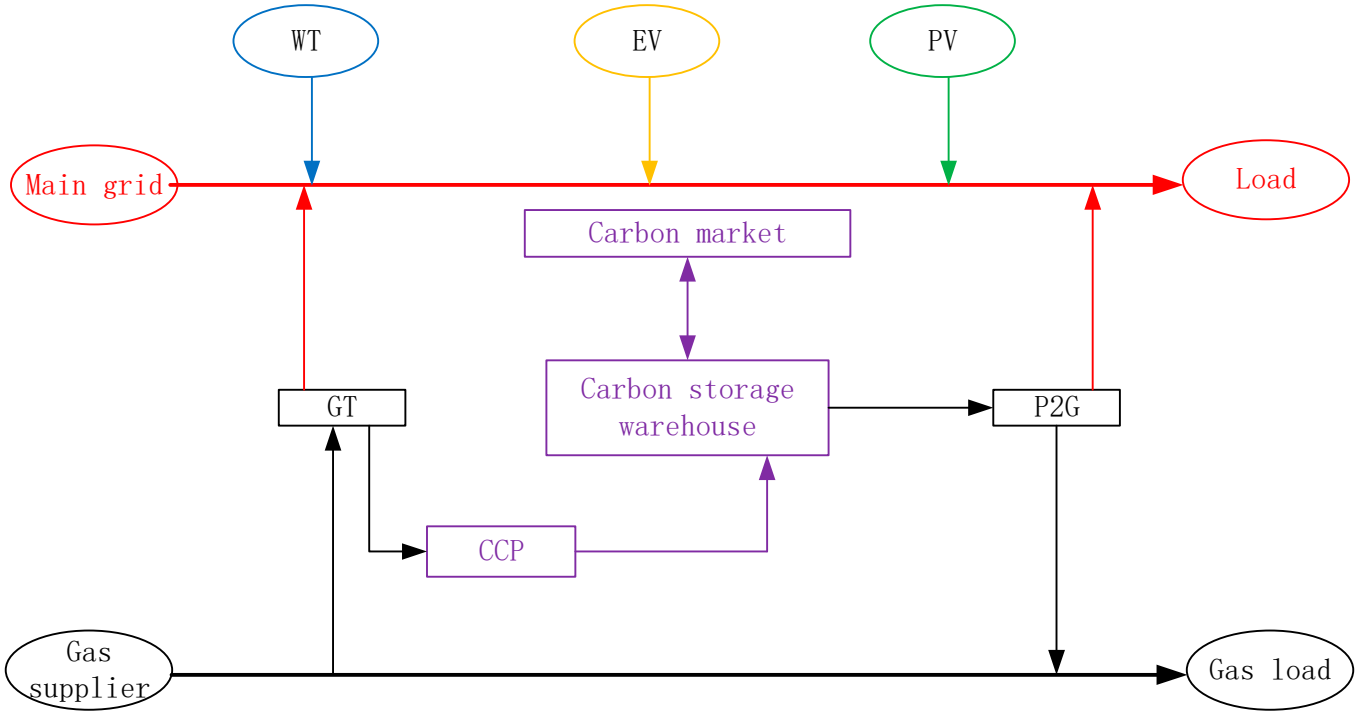

Figure 1. The structure of integrated electricity–gas distribution system.

3. Reliability Evaluation Method

In order to explore the impact of carbon trading price fluctuation on the total cost, this paper will consider the change in carbon selling price in the future.

4. Scheduling Model

4.1. Objective

On the basis of the operation of the traditional integrated distribution system, this paper analyses the operation of the V2G and IEGDS in the power grid for achieving low-carbon economical operation. The carbon emission tax and carbon market trading are also considered in this paper. The objective function, as shown in (1), is to get the minimum operating cost Z, which includes the distribution network operating cost (2), penalty cost of wind and PV power curtailment (3), natural gas system operating cost (4), carbon emission tax (5) and carbon trading cost (6).

$$minZ = \left(Z_E + Z_{loss} + Z_G + Z_f + Z_m\right) \tag{1}$$

$$Z_E = \sum_t {c_t}^E {P_t}^E \tag{2}$$

$$Z_{loss} = \sum_t {c_t}^{loss} {P_t}^{loss} \tag{3}$$

$$Z_G = \sum_t c_t^G G_t^S \tag{4}$$

$$Z_f = c_{tax} \sum_t \left(E_t^{ope} - E_t^L\right) \tag{5}$$

$$Z_m = c_b \sum_t E_t^{buy} - c_s \sum_t E_t^{sell} \tag{6}$$

4.2. Power Distribution System Constraints

4.2.1. The Travel Habits Constraints of Users

1. Charging start time of electric vehicle

Home time of the fuel car from NHTS (National Highway Traffic Safety Administration) can be used as the time when the electric vehicle plugs in, as shown in (7).

$$f_e(x) = \begin{cases} \frac{1}{\sqrt{2\pi}\sigma_e} \exp\left(-\frac{(x+24-\mu_e)^2}{2\sigma_e^2}\right) & 0 < x \le \mu_e - 12 \\ \frac{1}{\sqrt{2\pi}\sigma_e} \exp\left(-\frac{(x-\mu_e)^2}{2\sigma_e^2}\right) & \mu_e - 12 < x \le 24 \end{cases} \tag{7}$$

2. The daily mileage of private vehicle from NHTS

The daily mileage of private vehicle can be used as the daily power consumption of the EV, as shown in (8).

$$f_m(l) = \frac{1}{\sqrt{2\pi}\sigma_m l} \exp\left(-\frac{(\ln l - \mu_m)^2}{2{\sigma_m}^2}\right) \tag{8}$$

3. Next day departure time of electric vehicle

Next day departure time of the electric vehicle can be used the next day plug-out time of the EV, as shown in (9)

$$f_s(x) = \frac{1}{\sqrt{2\pi}\sigma_s} \exp\left(-\frac{(x-\mu_s)^2}{2\sigma_s^2}\right) \; 0 < x \le 24 \tag{9}$$

4.2.2. Electric Vehicle Charging Load Model

Cluster charging loads (10) for EVs are accumulated on the basis of individual charging loads for EVs.

$$P_{s,t} = \sum_{n=1}^{N} P_{n,t} \tag{10}$$

4.2.3. System Purchase Constraint from Substation

During the operation and dispatch of the system, the required power needs to be purchased from the converting station continuously. However, in order not to destroy the stability of the power network and consider the actual power supply capacity of the substation, the purchased power should be within the output size of the substation, which is shown in (11) and (12).

$$P_t^{E,\min} \le P_t^E \le P_t^{E,\max} \tag{11}$$

$$Q_t^{E,\min} \le Q_t^E \le Q_t^{E,\max} \tag{12}$$

4.2.4. The Constraints of System Node Voltage and Branch Current

Node voltage is one of the important indicators of power quality. Its stability is related to the quality and economy of the entire industrial production. Only when the system voltage (13) and current (14) are maintained at the normal level, can the major devices in the system operate normally and service life is not affected. Therefore, the operating system voltage and current must be within a certain range.

$$V_j^{\min} \le V_{jt} \le V_j^{\max} \tag{13}$$

$$I_{ij}^{\min} \le I_{ij,t} \le I_{ij}^{\max} \tag{14}$$

4.2.5. Output Limit of Wind Turbine and Wind Power Balance Constraints

Due to the influence of external factors such as power generation and wind speed of wind turbines, the output size of wind turbines is also limited similar to the substation (15). In the actual operation of the system, the absorbed wind power plus the abandoned wind power should be equal to the original wind power prediction power (16). The wind power and photoelectric processes are similar, and the predicted values are the portion that contains the actual output and shear load in (17) and (18).

$$0 \le P_{nt}^{WT} \le P_{nt}^{WT,F} \tag{15}$$

$$P_{nt}^{WT,F} = P_{nt}^{WT} + P_{nt}^{WT,loss} \tag{16}$$

$$0 \le P_{pt}^{PV} \le P_{pt}^{PV,F} \tag{17}$$

$$P_{pt}^{PV,F} = P_{pt}^{PV} + P_{pt}^{PV,loss} \tag{18}$$

4.2.6. Balance of Active and Reactive Power Flow

Power conservation must be observed in the operation of the power grid system. From the point of view of the whole system, the active and reactive power input of the power network should be the same as its active and reactive power consumption. Internally, the load power of each node should be equal to the sum of the power flowing into and out of the node. Using DistFlow power flow model constraints (19):

$$\begin{aligned} P_t^E = &- \sum_{n\in N(j)} P_{nt}^{WT} - \left(P_{ij,t} - I_{ij,t}^2 R_{ij}\right) - \sum_{p\in P(j)} P_{pt}^{PV} - \sum_{g\in G(j)} P_{gt}^{GT} + \sum_{c\in C(j)} P_{ct}^{C} \\ &+ \sum_{pg\in T(j)} P_{pgt}^{PtG} + \sum_{k\in K(j)} P_{jk,t} + \sum_{d\in D(j)} P_{dt}^{LD} - \sum_{d\in D(j)} P_{dt}^{loss} \end{aligned} \tag{19}$$

The load power of each node should be equal to the sum of the power flowing into and out of the node. GT flows into the current and P2G flows out of the gas storage station (20).

$$Q_t^E = \left(Q_{ij,t} - I_{ij,t}^2 X_{ij}\right) + \sum_{k \in K(j)} Q_{jk,t} + \sum_{d \in D(j)} Q_{dt}^{LD} - \sum_{d \in D(j)} P_{dt}^{loss} \cdot \varphi_{dt} \tag{20}$$

4.2.7. The Constraints Node Voltage Drop, Branch Current and Power Relationship

The voltage of each node is related to its surrounding voltage and the voltage of the branch, which is constrained by limiting the voltage of the node through the adjacent nodes and branches, as shown in (21).

$$V_{jt}^2 = V_{it}^2 - 2\left(P_{ij,t} R_{ij} + Q_{ij} X_{ij}\right) + I_{ij,t}^2 (R_{ij}^2 + X_{ij}^2) \tag{21}$$

Current is constrained by voltage through the node voltage, as well as by the relationship between power and current voltage (22).

$$I_{ij,t}^2 = (P_{ij,t}^2 + Q_{ij,t}^2)/V_{it}^2 \tag{22}$$

Both formulations are non-linear and non-convex, which results in a large amount of computation and high complexity in the optimization process. Therefore, in order to facilitate the solution, it is necessary to relax it to obtain a second-order cone optimization model.

$$\hat{V}_{jt} = \hat{V}_{it} - 2\left(P_{ij,t} R_{ij} + Q_{ij} X_{ij}\right) + \hat{I}_{ij,t}\left(R_{ij}^2 + X_{ij}^2\right) \tag{23}$$

$$\hat{I}_{ij,t} \geq (P_{ij,t}^2 + Q_{ij,t}^2)/V_{it}^2 \tag{24}$$

By further processing the above Formulas (23) and (24), the second order cone relaxation equation is obtained and the lower Equation (25) is obtained.

$$(2P_{ij,t})^2 + (2Q_{ij,t})^2 + (\hat{I}_{ij,t} - \hat{V}_{it})^2 \leq (\hat{I}_{ij,t} + \hat{V}_{it})^2 \tag{25}$$

where $\hat{I}_{ij,t} = I_{ij,t}^2$,$\hat{V}_{jt} = V_{jt}^2$, $\hat{V}_{it} = V_{it}^2$.

4.2.8. The Constraints of Charge and Discharge State

The (26)–(29) constraints determine the state of the electric vehicle during its participation in the orderly charge and discharge process:

$$I_{m,t}^{in} = I_{m,t}^{s} + I_{m,t}^{all} \tag{26}$$

$$I_{m,t}^{c} \leq I_{m,t}^{all} \tag{27}$$

$$I_{m,t}^{d} \leq I_{m,t}^{all} \tag{28}$$

$$I_{m,t}^{c} + I_{m,t}^{d} \leq 1 \tag{29}$$

4.2.9. The Constraints of Charge and Discharge Power

When the electric vehicle is charged as shown in (30), $I_{m,t}^{c} = 1$

$$0 \leq P_{m,t}^{c} \leq I_{m,t}^{c} P_{m}^{c,ra} \tag{30}$$

When the electric vehicle is discharged as shown in (31), $I_{m,t}^{d} = 1$

$$0 \leq P_{m,t}^{d} \leq I_{m,t}^{d} P_{m}^{d,ra} \tag{31}$$

4.2.10. The Constraints of the SOC

The initial SOC is equal to the SOC obtained at the time of access (32), and the SOC value at the time of leaving the power grid (33) should be the expected value.

$$-\left(1-I_{m,t}^{s}\right)M \le S_{m,t}-S_{m,0} \le \left(1-I_{m,t}^{s}\right)M \tag{32}$$

$$-\left(1-I_{m,t}^{e}\right)M \le S_{m,t}-S_{m,T} \le \left(1-I_{m,t}^{e}\right)M \tag{33}$$

4.2.11. The Constraints of Power Balance in Charge and Discharge Scheduling Process

The change of SOC in the state of charge at adjacent times must be equal to the SOC increment obtained from the charging or discharging power at the same time (34), that is, the charging or discharging power is balanced.

$$-\left(1-I_{m,t}^{all}\right)M \le \mathrm{S}_{m,t}-S_{m,(t-1)}-\frac{\eta_m^c P_{m,t}^c}{E_m}+\frac{P_{m,t}^d}{\eta_m^d E_m} \le \left(1-I_{m,t}^{all}\right)M \tag{34}$$

4.2.12. The Constraints of Gas Turbine Limits

Minimum start and stop time

$$\left(I_{j,t}^{GT}-I_{j,t-1}^{GT}\right)\left(U_{j,t-1}^{off}-T_j^{off,min}\right) \ge 0 \tag{35}$$

$$\left(I_{j,t}^{GT}-I_{j,t-1}^{GT}\right)\left(U_{j,t-1}^{on}-T_j^{on,min}\right) \ge 0 \tag{36}$$

4.2.13. The Constraints of Ramp

For the constraint of power generation at each moment, if the difference between the power required at the two moments is too large, and the gas turbine's power raising time exceeds this, it will not be able to meet the power demand, and the same at reducing power.

$$P_{j,t}^{GT}-P_{j,t-1}^{GT} \le R_j^u I_{j,t-1}^{GT}+P_j^{GT,min}\left(I_{j,t}^{GT}-I_{j,t-1}^{GT}\right)+P_j^{GT,max}\left(1-I_{j,t-1}^{GT}\right) \tag{37}$$

$$P_{j,t-1}^{GT}-P_{j,t}^{GT} \le R_j^d I_{j,t}^{GT}+P_j^{GT,min}\left(I_{j,t-1}^{GT}-I_{j,t}^{GT}\right)+P_j^{GT,max}(1-I_{j,t-1}^{GT}) \tag{38}$$

4.3. The Constraints of Gas Distribution Network

4.3.1. Gas System Balance Constraints

Similar to the system power flow constraint, it ensures that the natural gas flow at each node is within the normal range (39), and the demand for natural gas at each node of the system is met.

$$\sum_{o\in N(n)} G_{no,t}-G_{xy,t}=G_{s,t}^{S}-\sum_{(m,n)\in\Omega^c}\eta_{xy}G_{xy,t}+G_{pg,t}^{PtG}-G_{g,t}^{GT}-G_{l,t}^{LD} \tag{39}$$

4.3.2. Weymouth Model

At t this moment, the node needs to meet a certain gas pressure to ensure the normal flow of gas in the natural gas system, as shown in (40) and (41).

$$G_{xy,t}=K_{xy}\sqrt{\left(\pi_{x,t}^2-\pi_{x,t}^2\right)},(x,y)\in\Omega^P \tag{40}$$

The gas pressure at the next node is determined by the gas pressure at the previous node and the compression coefficient of the compressor (47). The reason why the gas pressure is less, is because there is loss in the pipeline.

$$\pi_{x,t}\le\tau_{xy}\pi_{x,t},(x,y)\in\Omega^C \tag{41}$$

4.3.3. The Constraints of Coupling

The constraints of a gas turbine as an electrically coupled device. The natural gas consumption function $f\left(P_{j,t}^{GT}\right)$ is related to the actual output of the gas turbine and is summarized as follows (42):

$$\left(P_{j,t}^{GT}\right) = a_j\left(P_{j,t}^{GT}\right)^2 + b_j P_{j,t}^{GT} + c_j \tag{42}$$

Start-Stop

The gas turbine can only be started when the cost is met which is shown in (43)–(45)

$$C_{j,t}^{up} \geq c_j^{up}\left(I_{j,t}^{GT} - I_{j,t-1}^{GT}\right), C_{j,t}^{up} \geq 0 \tag{43}$$

$$C_{j,t}^{down} \geq c_j^{down}\left(I_{j,t-1}^{GT} - I_{j,t}^{GT}\right), C_{j,t}^{down} \geq 0 \tag{44}$$

$$G_{g,t}^{GT} = \left(f\left(P_{j,t}^{GT}\right) + C_{j,t}^{up} + C_{j,t}^{down}\right)/HHV \tag{45}$$

4.3.4. The Operating Constraints of P2G

P2G is one of the important parts of IEGDS, especially when there are a quantity of WTs and PVs. When there is too much power which cannot be fully absorbed by the IEGDS shown in (46), the excess power will be stored by the P2Gs. Normally, P2G efficiency is roughly in the range of 50–70%, and the high heat value HHV = 1.026 MBth/kcf, and energy conversion factor φ = 3.4 MBtu/MWh.

$$G_{n,t}^{PtG} = \frac{\phi\eta_j^{PtG} P_{n,t}^{PtG}}{HHV} \tag{46}$$

During the conversion process, the P2Gs equipment needs to consume energy. This Formula (47) ensures whether the P2G equipment is turned on or not.

$$I_{j,t}^{PtG} + I_{j,t}^{GT} = 1, where\ PtG, GT\ at\ node\ j \tag{47}$$

4.3.5. The Network Constraints of Natural Gas

Similar to Formula (48), in Weymouth's case it is the overall constraint on the natural gas network:

$$(G_{mn,t})^2 + \left(K_{mn}\pi_{n,t}\right)^2 \leq \left(K_{mn}\pi_{m,t}\right)^2, (m,n) \in \Omega^P \tag{48}$$

4.4. The Constraints of Carbon Emission

4.4.1. The Constraints of IEGDS

Break our free carbon quota from the carbon market into two parts, one for the main grid of electric vehicles (49) and one for the gas (50).

$$E_t^{L,mg} = \varepsilon^{mg} \sum_{j \in \Omega^T} P_{j,t}^{mg} \tag{49}$$

$$E_t^{L,GT} = \varepsilon^{gt} \sum_{j \in \Omega^T} P_{j,t}^{GT} \tag{50}$$

4.4.2. The Constraints of Carbon Emission and Carbon Collection

$$E_{j,t}^{mg} = e^{mg} P_{j,t}^{mg} \tag{51}$$

$$E_{j,t}^{GT} = e^{gt} P_{j,t}^{GT} \tag{52}$$

The following constraints (53) apply to the efficiency of carbon collection and gas turbine emissions

$$0 \leq E_{j,t}^{ccp} \leq \zeta E_{j,t}^{GT} \tag{53}$$

The total power loss during the carbon emission collection process (54) is divided into two parts, one part is fixed loss, the other part is operational power loss and changes with the amount of carbon captured.

$$P_{j,t}^{c} = P_{j,t}^{fix} + \eta^{ccp} E_{j,t}^{ccp} \tag{54}$$

4.4.3. The Constraints of Carbon Utilization

In the process of carbon neutrality, the primary purpose is to reduce carbon emissions, so carbon capture and carbon storage are involved in this process; first, the capture and then the storage. When the storage reaches a certain limit (55), transport this part of carbon to IEGDS, and then use P2G to transform this part of carbon.

$$M_{j,t}^{ct} = M_{j,t-1}^{ct} + E_{j,t}^{ccp} - M_{j}^{ct,max} I_{j,t}^{ct,dep} \tag{55}$$

The following Formula (56) expresses the balance constraint of the carbon storage warehouse:

$$M_{j,t}^{cs} = M_{j,t-1}^{cs} + M_{t}^{cs,in} - M_{t}^{cs,out} + M_{j}^{ct,max} I_{j,t}^{ct,arr} \tag{56}$$

The following Formula (57) expresses the consumption of carbon dioxide during P2G operation

$$E_{j,t}^{PtG} = \rho_{j}^{PtG} P_{j,t}^{PtG} \tag{57}$$

4.4.4. The Constraints of Carbon Trade

In the model of this paper, the carbon trade (58) is divided in two parts, the first one is based on the part free carbon emission tax trade, the second one is carbon trading income and expenditure.

$$M_{j,t}^{cs} + E_{t}^{sell} + \sum_{j \in \Omega^{PtG}} E_{j,t}^{PtG} = M_{t}^{cs,out} + E_{t}^{buy} \tag{58}$$

5. Case Study

5.1. Case Study Introduction

To test the validity of this example, the IEEE 33-node diagram and a modified 20-node Belgian gas network [23] are used in this paper (Figure 2). In the whole system, this paper uses 3WTs, 2 PVs, 3 P2Gs, 2 EV clusters and two GTs. The main grid is powered by the substation located at Node 1. For the sake of integrated cost and more convenient access of electric vehicles, this paper uses a time-sharing electricity price, which is shown in Table 1 as different time electricity price costs. In the process of EV access, the clustering of EVs is processed in this paper, and half of the total number of EVs connected at Nodes 5 and 15 of the main grid are subject to active and ordered scheduling. For WTs and PVs, photoelectric and wind power output are shown in Figure 3.

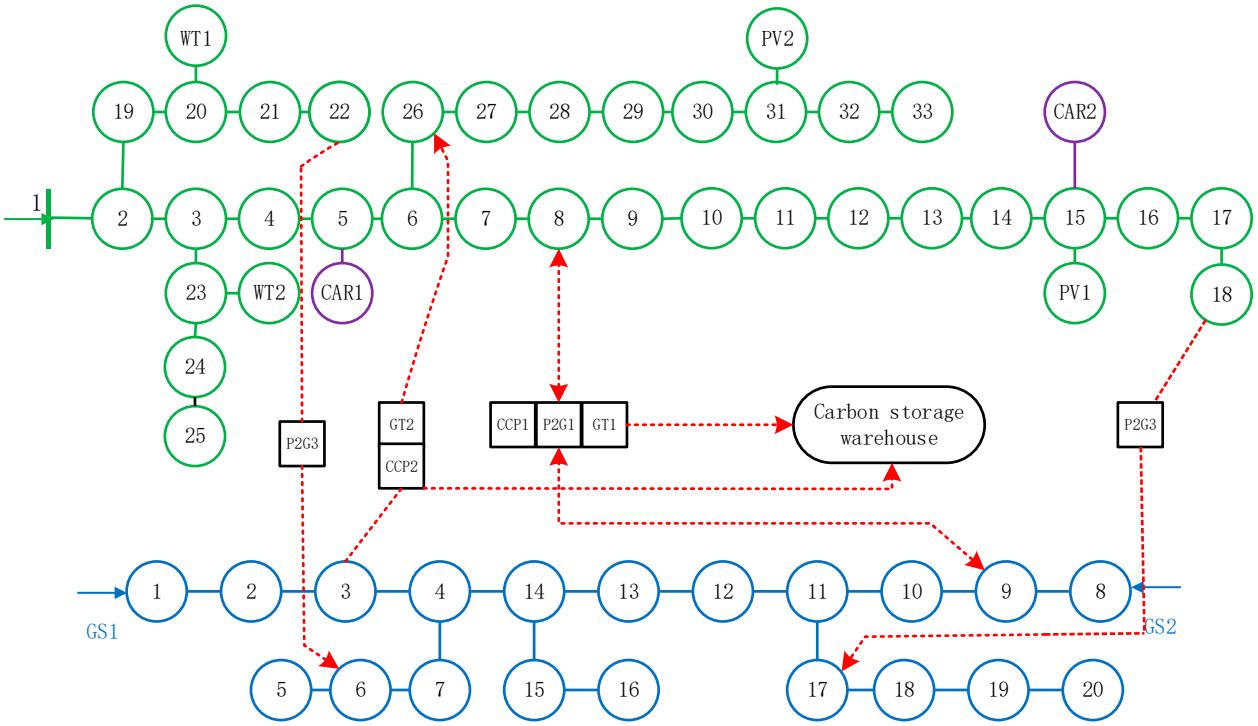

Figure 2. The IEEE 33-node electricity distribution grid and 20-node Belgian gas network.

Table 1. Time-of-use electricity price.

	Time (h)	Price (CNY)
Peak period	12–14, 18–20	2.83
Normal period	8–11, 14–17, 21–23	1.67
Valley period	0-7	0.58

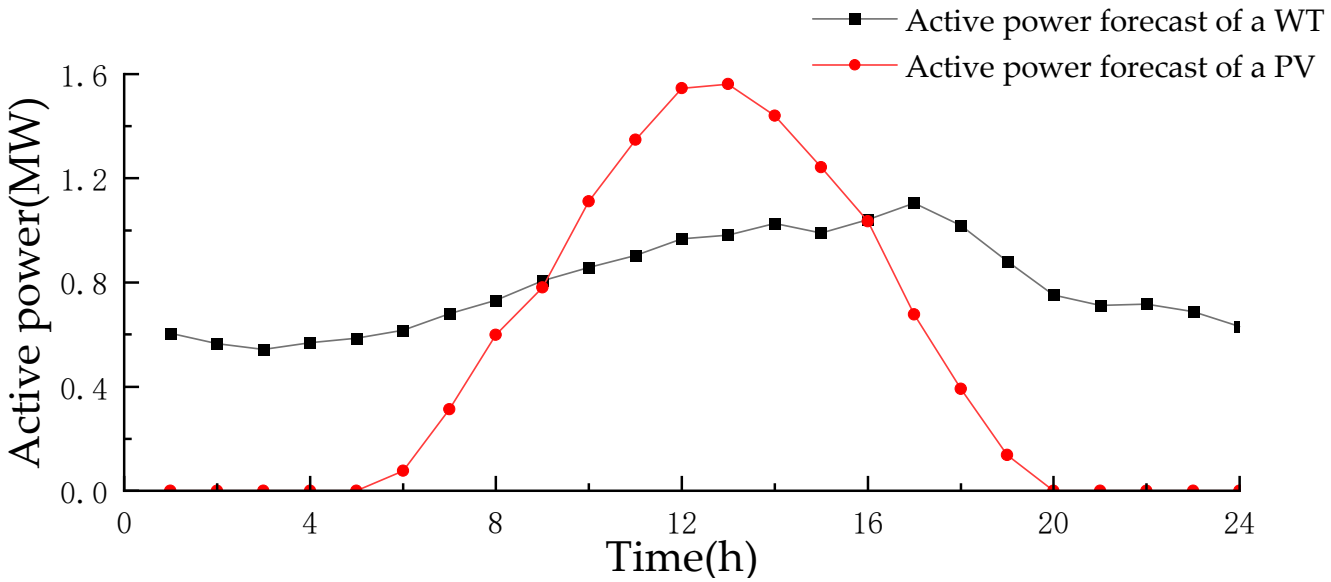

Figure 3. Power generation forecast of WT/PV.

For the gas network, this paper uses gas nodes 1 and 8 to supply the gas network, including 2 compressors, 17 pipelines and 13 gas loads. The maximum capacities of the GTs are 2MW. The maximum input power of P2Gs is 0.8 MW, and the conversion efficiency

of P2Gs is 0.64. The maximum output of gas suppliers at nodes 1 and 8 are 22 kcf/h and 25 kcf/h, natural gas prices are set to 10.8 ¥/kcf, 12.6 ¥/kcf, respectively. During the carbon trading process, we designed the carbon storage tank around the CCP unit and designed a capacity of 0.9 tons for it. Carbon is transported to the carbon storage warehouse by electric truck, the maximum capacity of the carbon storage warehouse is 10 tons, and its maximum input and output limit are 3 tons/h, and the maximum amount of carbon to be bought and sold in each period is 1 ton.

During the process of carbon emission, the power generation in the main grid is set to 0.96 t/MW, and for natural gas power generation, the carbon emission of the gas turbine is set to 0.65 t/MW. Consider renewable energy generating units as zero carbon emissions. In this paper, the gas turbine is transformed into a carbon capture plant, with a carbon capture rate of 84% and a power consumption factor of 0.269 MW/t. The carbon emission quota for the main grid and gas turbines are 0.53 and 0.32 t/MW, respectively. In the carbon market, at first, the carbon emission tax is 25 ¥/t. The following is an example analysis.

5.2. The Influence of Different Access Cases of Electric Vehicles on Load

Under the condition that the gas network load is normal and the gas turbine is started, in the basic load of the power grid as shown in Figure 4, half of the total number of electric vehicles are connected at nodes 5 and 15 in this paper, which can clearly see the impact of electric vehicles on the total load of the power grid. In order to explore the impact of electric vehicles on the operation of the power grid, this paper sets the number of electric vehicles as 800 and 1200, respectively, The comparison is made under the condition of orderly access and disordered access of electric vehicles. Disorderly access of electric vehicles is adopted in Case 1. X, orderly charge of electric vehicles is adopted in Case 2. X. The number of electric vehicles is shown in Table 2, where: "×" means that the number is not used in case; "√" means that the number is used in case.

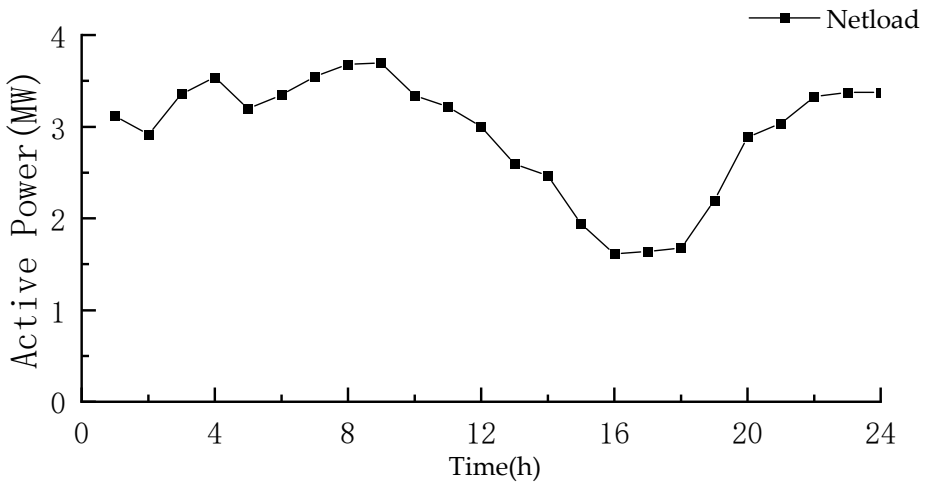

Figure 4. The net load forecast.

Table 2. The different cases in V2G.

Electric Vehicles Number	Case 1.1	Case 1.2	Case 2.1	Case 2.2
800	√	×	√	×
1200	×	√	×	√

Figure 5 describes the comparison chart of net load of electric vehicles connected to the power grid in order and disorder. Table 3 shows the different costs when only electric vehicles are connected to the gas network of the power grid. Compared with Case 1.1, Case 1.2 increases the load during the peak period of power consumption, and puts forward more stringent requirements for grid dispatching, which is consistent with the

increase under the condition that more electric vehicles are connected. Compared with Case 1.1, Case 2.1 can clearly see the role of "peak shaving and valley filling". In the original peak period of electricity use, the net conformity of the power grid from 7:00 to 12:00 has obviously shifted to the low valley of electricity use from 12:00 to 20:00. The peak valley difference of net load has decreased by 0.80469 MW, and the cost has decreased by 3.46366 yuan. It can also be clearly seen that with the increase of the number of electric vehicles connected, the phenomenon of "peak cutting and valley filling" is more obvious, the cost is reduced more, which increases the controllability of electric vehicles, effectively prevents electric vehicles from charging in peak hours, making the power grid safer and the allocation more stable. With the increase of access, its positive role is more obvious. However, in this paper, the electric vehicle plays the role of cutting the peak and filling the valley. It has limited contribution to the renewable energy consumption, so P2G equipment is introduced.

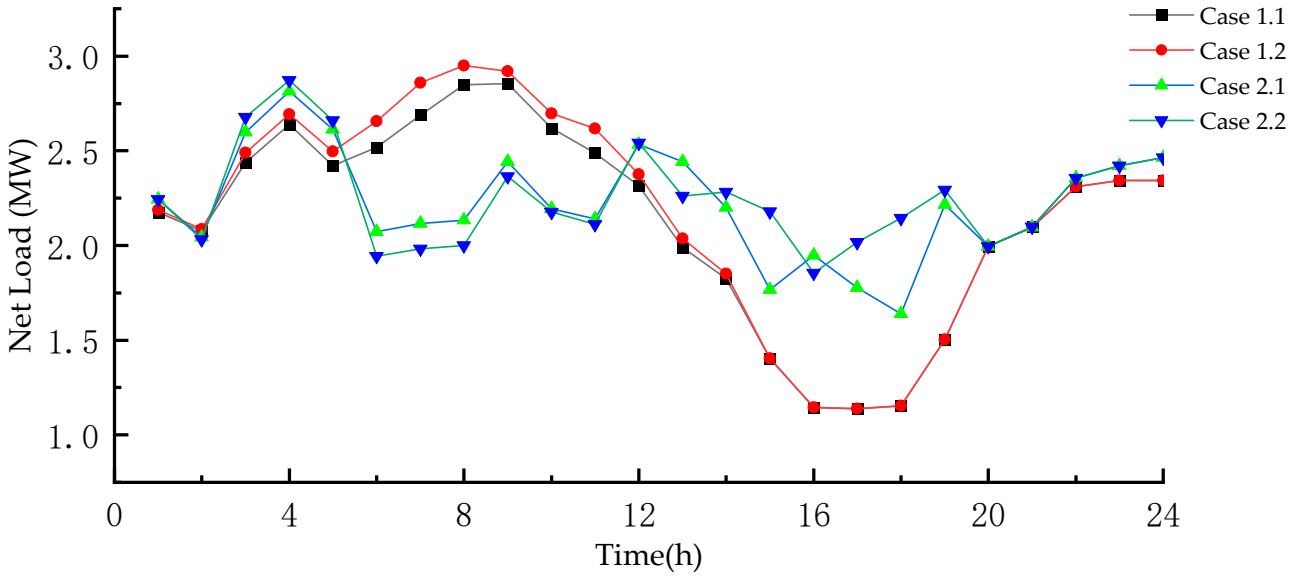

Figure 5. Net load with different cases.

Table 3. The different cost between different cases.

Case	Case 1.1	Case 1.2	Case 2.1	Case 2.2
Cost (CNY)	7414.52	7417.07	7411.05	7410.50

By observing Table 3 and comparing Case1.1 with Case1.2, we can get that the EV for renewable energy consumption has increased after the increase of EVs, which makes the cost increase not much; comparing Case2.1 with Case2.2, we can also see that the total system cost reduction is limited after the EVs are connected to the grid in an orderly manner, in fact it is net load shaving and valley filling, which changes the EV charging time in The cost reduction is limited after the number of EVs increases, but the net load shedding is more obvious.

5.3. The Influence of Different Access Cases of Electric Vehicles on Load

In order to explore the impact of P2G devices on renewable energy consumption, this paper introduces P2G devices to get Case 3 on the basis of Case 2.1. On the basis of Case 3, the following settings are made considering the impact of different number of EVs on P2G elimination EVs.

Case 3.1 Considering V2G with 800 EVs

Case 3.2 Considering V2G with 1200 EVs

Figure 6 shows the total of wind and PV curtailment. From Figure 6, it can be seen that Case 3.1 has a significant improvement on renewable energy consumption after considering P2G devices. By comparing Case 2.1 and Case 3.1, it can be explored that during the period of 8:00–18:00 when wind and PV curtailment was most, the absorbability has been significantly improved, and the absorbance has a maximum improvement of 0.414 MW; the effect is obvious, and effectively improves the system's ability to consume renewable energy. By comparing Case 3.1 and Case 3.2, we can see that P2G devices and their own EV consumption have no impact, but the EV cluster's ability to consume renewable energy is limited.

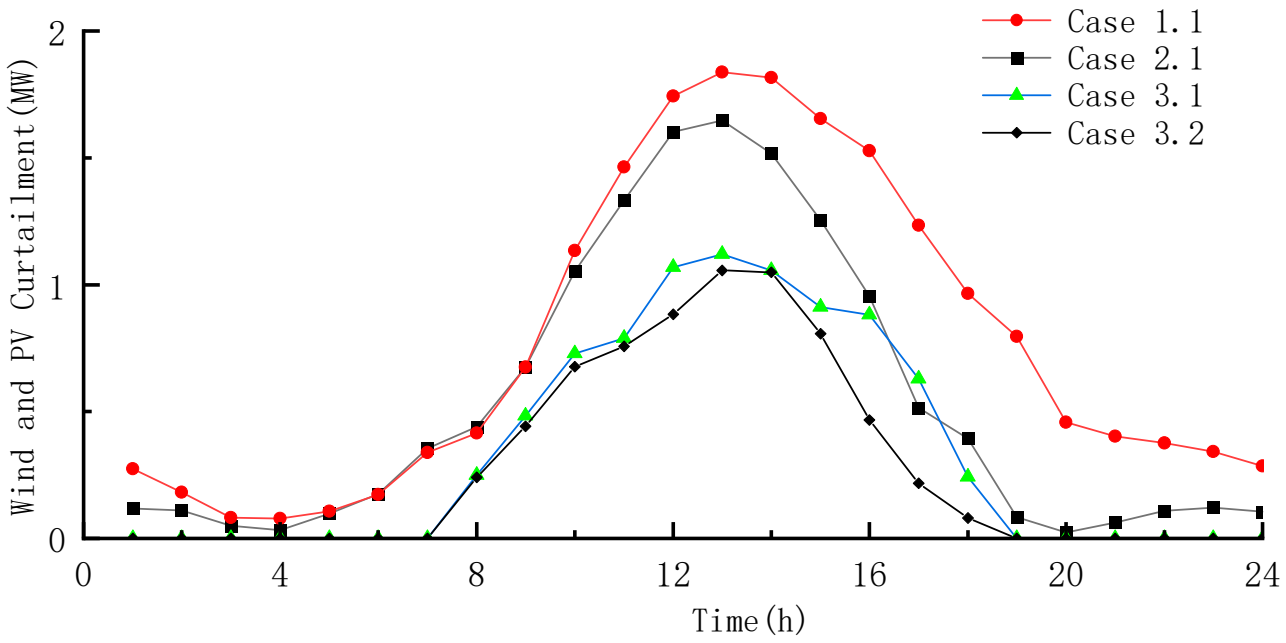

Figure 6. Wind and PV curtailment in Case 3.

In Figure 7, after P2G equipment is connected, the cost of the whole system has decreased significantly. After the consumption of renewable energy has increased, the total cost has decreased by 1669.79 yuan. After more renewable energy has been consumed and converted into natural gas, the gas purchase price has decreased significantly, reaching 1445.64167 yuan. P2G equipment has reduced the cost by converting renewable energy with lower cost into natural gas with higher cost.

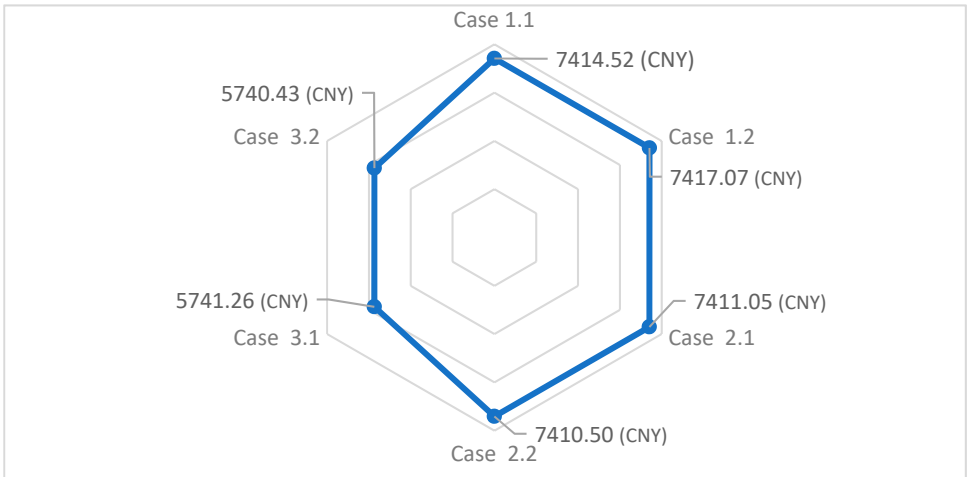

Figure 7. All costs in the different cases.

5.4. Systematic Overall Impact Considering Carbon Emission Markets

To explore the role of carbon capture devices in the whole system, carbon capture devices are set up in electrical nodes 8 and 26, where CCP1 can directly supply CO_2 to P2G1. In order to analyze the impact of the introduction of carbon capture devices on the operation of the whole system, a carbon trading market is introduced in Case 4.

Case 4.1 is based on Case 3.1 and the carbon market price is the selling price of carbon is 31 ¥/t, and the buying price of carbon is 35 ¥/t.

Case 4.2 changes the selling price of carbon to 35 ¥/t and the buying price of carbon is 35 ¥/t in Case 4.1.

Case 4.3 changes the selling price of carbon to 27 ¥/t and the buying price of carbon is 35 ¥/t in Case 4.1.

Figure 8 considers the total carbon emission of all cases in the carbon trading market. From Figure 8, it can be seen that the total carbon emission of the system decreases greatly after the introduction of the carbon trading market. It can be seen that during the optimization process, both EV and P2G increase the total carbon emission of the system. After the addition of the carbon capture device, the total carbon emission of the system decreases greatly, with the maximum difference reaching 26.7226 t, the effect is obvious. By comparing Case 4.1 and Case 4.2, it is found that increasing the selling price of carbon will have less influence on the overall carbon emission of the system when the purchased carbon is unchanged. By comparing Case 4.1 with Case 4.3, it will affect the total amount of carbon capture and increase the total amount of carbon emissions when reducing the selling price of carbon. Therefore, Case 4.1 is a better option in the carbon trading market.

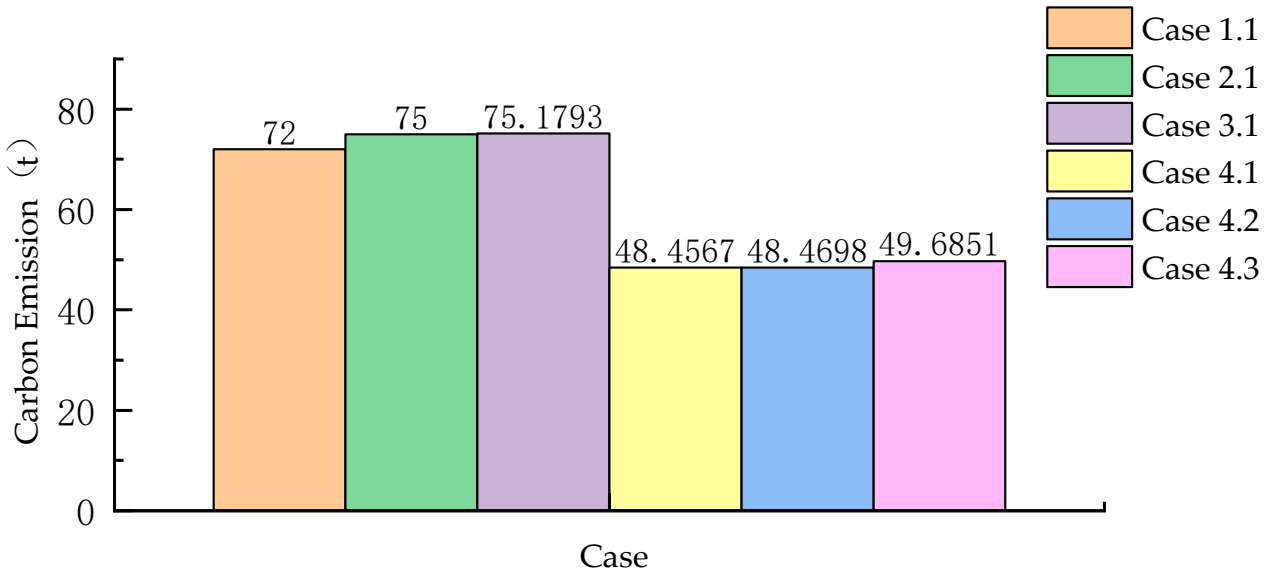

Figure 8. Carbon emission of different cases.

The negative number in Table 4 is the profit cost. By comparing the costs in Table 4, the total cost of Case 4.1 and Case 4.2 differs by 100 yuan when the selling price differs by only 4 yuan, which is considerable for the total cost of the system. So, in Figure 8, Table 4, if the difference between Case 4.1 and Case 4.2 is not big, selling at a higher carbon cost is beneficial to the cost control of the system. To sum up, when the selling price of carbon increases positively, the carbon emissions of the system are almost unchanged, the cost is reduced, the carbon emissions increase when the selling price is lower, and the total cost increases at the same time.

Table 4. The different cost between Case 4.x.

Running Case	Power Purchase Cost (CNY)	Gas Purchase Cost (CNY)	Carbon Trade Cost (CNY)	Total Cost (CNY)
Case 4.1	77.42	6680.47	−657.59	6363.27
Case 4.2	63.02	6680.47	−745.39	6261.14
Case 4.3	65.53	6660.39	−564.72	6437.97

6. Conclusions

In view of the low-carbon scheduling of integrated electricity and gas distribution system considering V2G, this paper has established a basic gas electricity interconnection system, including the orderly dispatch of electric vehicles based on P2G equipment and carbon storage equipment, combined carbon capture, carbon storage and low carbon economic dispatch with fluctuating carbon prices, and obtained an effective model through numerical example analysis. The conclusions are as follows:

(1) After considering the orderly dispatching of electric vehicles, the electric vehicles are guided to actively participate in orderly charging and discharging, and are connected to the power grid for charging when the net load is small at the low price valley, which realizes peak shaving and valley filling, and increases the security, economy and efficiency of energy storage of the power grid.
(2) After the P2G devices are connected, the multi-energy complementary capacity of the system is significantly improved, the energy conversion efficiency is further enhanced, and the dispatching of main grid is more flexible and convenient.
(3) Taking into account the electric vehicle access, the P2G equipment is connected to the electrical interconnection system, which has significantly improved the renewable energy consumption of the power grid, the high proportion of renewable energy consumption capacity of the whole system, and significantly reduced the cost.
(4) After considering the carbon trading market, the implementation effect of low-carbon economy for the whole system is obvious, and the overall carbon emissions of the system are greatly reduced. Considering the fluctuation of carbon price, a better carbon trading case is obtained. Considering the overall planning of carbon storage, carbon emissions and transportation trading links, the total cost of the system can be controlled to obtain the lowest cost, along with the fluctuation of the carbon trading price.

Author Contributions: Conceptualization, L.X.; Data curation, Y.L. and X.L.; Funding acquisition, L.X.; Investigation, Y.L. and Y.X.; Methodology, Y.L.; Software, Y.L.; Validation, Y.L.; Writing—original draft, Y.L.; Writing—review & editing, L.X. All authors have read and agreed to the published version of the manuscript.

Funding: There is no funding in this paper.

Data Availability Statement: Data available on request from the authors.

Conflicts of Interest: The authors declare no conflict of interest.

Nomenclature

Indices	
t	Index of hours
j,(i,j),d	Index of voltage node/current of branch/load
n, p	Index of wind power/PV node
pg	Index of P2G node
Variables:	
Z	All costs of the system

Z_E	The distribution network operating cost
Z_{loss}	The penalty cost of WT and PV power curtailment
Z_G	The natural gas system operating cost
Z_f	The carbon emission tax
Z_m	The carbon trading cost
${P_t}^E$	The active power from main grid at time t;
$P_{ij,t}$	The active power from main grid at time t of power line (i,j)
${P_t}^W / {P_t}^{PV}$	The active power of WT/PV at time t
${P_t}^{loss}$	The active loss power at time t
$P_{m,t}^{c,ra} / P_{m,t}^{d,ra}$	Order to charge and discharge the rated power of electric vehicles
$P_{nt}^{WT} / P_{pt}^{PV}$	The active power of WT/PV at time t at node n/p
$P_{nt}^{WT,F} / P_{pt}^{PV,F}$	Forecast active power of WT/PV at time t at node n/p
$P_{nt}^{WT,loss} / P_{pt}^{PV,loss}$	Loss active power of WT/PV at time t at node n/p
$P_{j,t}^{GT} / Q_{j,t}^{GT}$	Active/reactive power generation of GT at node j at time t
$P_{j,t}^{c} / P_{j,t}^{fix}$	Power consumption, and fixed power consumption of CCP at node j at time t
Q_t^E	Reactive power from main grid at time t
$Q_{ij,t}$	Reactive power from main grid at time t of power line (i,j)
E_t^{ope}	Actual system carbon emission at time t
E_t^L	Total free carbon quota at time t
E_t^{buy} / E_t^{sell}	Carbon bought and sold in carbon market at time t
$E_{j,t}^{ccp}$	The amount of carbon being captured at node j at time t
$E_{j,t}^{GT}$	Carbon production of GT at node j at time t
$E_{j,t}^{PtG}$	Carbon production of P2G at node j at time t
E_t^{sell} / E_t^{buy}	Carbon bought and sold in carbon market at time t
V_{jt}	Node voltage at node j at time t
$I_{ij,t}$	Current of branch (i,j) at time t
$I_{m,t}^{in}$, $I_{m,t}^{s}$, $I_{m,t}^{all}$, $I_{m,t}^{c}$, $I_{m,t}^{d}$	Binary 0 and 1 variables that represent the state.
$I_{m,t}^{in}$	Whether the electric vehicle is connected to the grid at time t, yes is 1, otherwise is 0
$I_{m,t}^{s}$	Indicate whether the electric vehicle is connected to the grid at time t
$I_{m,t}^{all}$	Indicate whether the electric vehicle is available for charging and discharging at time t
$I_{m,t}^{c}$	Indicate the charging state of the electric vehicle, only when charging is 1
$I_{m,t}^{d}$	Indicate the discharging state of the electric vehicle, 1 when discharging only
$I_{j,t}^{GT} / I_{j,t}^{P2G}$	Status indicator that is equal to 1 if GT/P2G at node j is online at time t
$S_{m,t}$	The SOC size of the electric vehicle at time t
$S_{m,0}$	The SOC size at the time of connection to the grid
E_m	Electric vehicle battery capacity
$G_{n,t}^{PtG} / G_{n,t}^{S}$	Gas output of P2G/gas supplier at node n at time t
$G_{n,t}^{LD} / G_{n,t}^{GT}$	Gas demand of gas load/GT at node n at time t
$S_{m,T}$	The expected SOC size at the time of leaving the grid, respectively
$M_{j,t}^{ct} / M_{j,t}^{cs}$	Capacity of carbon storage tank/carbon storage warehouse at node j at time t
$M_t^{cs,in} / M_t^{cs,out}$	Input/output of carbon storage warehouse at time t
Parameters	
${c_t}^E / c_t^G$	The price of electricity/natural gas at time t
${c_t}^{loss}$	The penalty price of WT and PV power curtailment
c_{max}	The price of carbon emission tax
c_b / c_s	The price of purchase/selling CO_2
$C_{j,t}^{up} / C_{j,t}^{down}$	Startup/shutdown cost of GT at node j at time t
R_{ij} / X_{ij}	Resistance/reactance of power line (i,j)

γ	Penalty coefficient of nodal pressure
$\pi_{x,t}$	Gas pressure at time t at node x
Ω^P	Set of pipelines
μ	Mathematical expectations
σ	Standard deviation
ζ	Carbon capture rate of CCP
M	One infinite large positive number
ρ_j^{PtG}	Carbon consumption per unit of electricity in P2G at node
K_{xy}	Gas flow constant of gas pipeline (x,y)
τ_{xy}	Compressor factor at pipeline (x,y)
η_m^c / η_m^d	Electric vehicle charging and discharging efficiency
$\varepsilon^{mg} / \varepsilon^{gt}$	Carbon emission quota per unit of main grid/GT
e^{mg} / e^{gt}	Carbon emission intensity of main grid/GT

References

1. Xu, B.; Chen, J. How to achieve a low-carbon transition in the heavy industry? A nonlinear perspective. *Renew. Sustain. Energy Rev.* **2021**, *140*, 110708. [CrossRef]
2. Javadi, M.A.; Khodabakhshi, S.; Ghasemiasl, R.; Jabery, R. Sensivity analysis of a multi-generation system based on a gas/hydrogen-fueled gas turbine for producing hydrogen, electricity and freshwater. *Energy Convers. Manag.* **2021**, *252*, 115085. [CrossRef]
3. Tang, C.; Liu, M.; Liu, Q.; Dong, P. A per-node granularity decentralized optimal power flow for radial distribution networks with PV and EV integration. *Int. J. Electr. Power Energy Syst.* **2019**, *116*, 105513. [CrossRef]
4. Javadi, M.; Najafi, N.J.; Abhari, M.K.; Jabery, R.; Pourtaba, H. 4E analysis of three different configurations of a combined cycle power plant integrated with a solar power tower system. Sustain. *Energy Technol. Assess.* **2021**, *48*, 101599.
5. Jin, B. Research on performance evaluation of green supply chain of automobile enterprises under the background of carbon peak and carbon neutralization. *Energy Rep.* **2021**, *7*, 594–604. [CrossRef]
6. Wang, S.; Dong, Z.Y.; Chen, C.; Fan, H.; Luo, F. Expansion Planning of Active Distribution Networks With Multiple Distributed Energy Resources and EV Sharing System. *IEEE Trans. Smart Grid* **2019**, *11*, 602–611. [CrossRef]
7. Zeng, Z.; Ding, T.; Xu, Y.; Yang, Y.; Dong, Z.Y. Reliability Evaluation for Integrated Power-Gas Systems With Power-to-Gas and Gas Storages. *IEEE Trans. Power Syst.* **2019**, *35*, 571–583. [CrossRef]
8. Zhang, F.; Salimu, A.; Ding, L. Operation and optimal sizing of combined P2G-GfG unit with gas storage for frequency regulation considering curtailed wind power. *Int. J. Electr. Power Energy Syst.* **2022**, *141*, 108278. [CrossRef]
9. Chen, Y.; Guo, Q.; Sun, H.; Pan, Z.; Chen, B. Generalized phasor modeling of dynamic gas flow for integrated electricity-gas dispatch. *Appl. Energy* **2020**, *283*, 116153. [CrossRef]
10. Correaposada, C.M.; Sanchez-Martan, P. Gas Network Optimization: A Comparison of Piecewise Linear Models. 2014. Available online: https://optimization-online.org/2014/10/4580/ (accessed on 10 October 2014).
11. Bent, R.; Blumsack, S.; Van Hentenryck, P.R.; Borraz-Sanchez, C.; Shahriari, M. Joint Electricity and Natural Gas Transmission Planning With Endogenous Market Feedbacks. *IEEE Trans. Power Syst.* **2018**, *33*, 6397–6409. [CrossRef]
12. Wu, G.; Li, T.; Li, M.; Lan, P.; Ma, R.; Ma, T.; Jingwei, D. Day-ahead optimal scheduling model of transmission–distribution integrated electricity–gas systems based on convex optimization. *Energy Rep.* **2022**, *8*, 759–767. [CrossRef]
13. He, C.; Zhang, X.; Liu, T.; Wu, L. Distributionally Robust Scheduling of Integrated Gas-Electricity Systems with Demand Response. *IEEE Trans. Power Syst.* **2019**, *34*, 3791–3803. [CrossRef]
14. Alabi, T.M.; Lu, L.; Yang, Z. Data-driven optimal scheduling of multi-energy system virtual power plant (MEVPP) incorporating carbon capture system (CCS), electric vehicle flexibility, and clean energy marketer (CEM) strategy. *Appl. Energy* **2022**, *314*, 118997. [CrossRef]
15. Wang, J.; Wu, Z.; Du, E.; Zhou, M.; Li, G.; Zhang, Y. Constructing a V2G-enabled regional energy Internet for cost-efficient carbon trading. *CSEE J. Power Energy Syst.* **2020**, *6*, 31–40.
16. Wei, X.; Sun, Y.; Zhou, B.; Zhang, X.; Wang, G.; Qiu, J. Carbon emission flow oriented multitasking multi-objective optimization of electricity-hydrogen integrated energy system. *IET Renew. Power Gener.* **2022**, *16*, 1474–1489. [CrossRef]
17. Fambri, G.; Diaz-Londono, C.; Mazza, A.; Badami, M.; Sihvonen, T.; Weiss, R. Techno-economic analysis of Power-to-Gas plants in a gas and electricity distribution network system with high renewable energy penetration. *Appl. Energy* **2022**, *312*, 118743. [CrossRef]
18. Gu, C.; Zhang, Y.; Wang, J.; Li, Q. Joint planning of electrical storage and gas storage in power-gas distribution network considering high-penetration electric vehicle and gas vehicle. *Appl. Energy* **2021**, *301*, 117447. [CrossRef]
19. Ju, L.; Yin, Z.; Lu, X.; Yang, S.; Li, P.; Rao, R.; Tan, Z. A Tri-dimensional Equilibrium-based stochastic optimal dispatching model for a novel virtual power plant incorporating carbon Capture, Power-to-Gas and electric vehicle aggregator. *Appl. Energy* **2022**, *324*, 119776. [CrossRef]
20. Cao, J.; Crozier, C.; McCulloch, M.; Fan, Z. Optimal Design and Operation of a Low Carbon Community Based Multi-Energy Systems Considering EV Integration. *IEEE Trans. Sustain. Energy* **2018**, *10*, 1217–1226. [CrossRef]

21. Zhang, Z.; Du, J.; Zhu, K.; Guo, J.; Li, M.; Xu, T. Optimization scheduling of virtual power plant with carbon capture and waste incineration considering P2G coordination. *Energy Rep.* **2022**, *8*, 7200–7218. [CrossRef]
22. Wei, H.; Zhang, Y.; Wang, Y.; Hua, W.; Jing, R.; Zhou, Y. Planning integrated energy systems coupling V2G as a flexible storage. *Energy* **2021**, *239*, 122215. [CrossRef]
23. Zhang, G.; Wang, W.; Chen, Z.; Li, R.; Niu, Y. Modeling and optimal dispatch of a carbon-cycle integrated energy system for low-carbon and economic operation. *Energy* **2022**, *240*, 122795. [CrossRef]
24. Wang, L.; Shi, Z.; Dai, W.; Zhu, L.; Wang, X.; Cong, H.; Shi, T.; Liu, Q. Two-stage stochastic planning for integrated energy systems accounting for carbon trading price uncertainty. *Int. J. Electr. Power Energy Syst.* **2022**, *143*, 108452. [CrossRef]
25. Song, X.; Wang, P.; Zhang, B.; Xing, T. A low-carbon peak-load regulation trading strategy for large-scale wind power integration using information gap decision theory. *Energy Rep.* **2022**, *8*, 9642–9661. [CrossRef]
26. Nie, Q.; Zhang, L.; Tong, Z.; Dai, G.; Chai, J. Cost compensation method for PEVs participating in dynamic economic dispatch based on carbon trading mechanism. *Energy* **2021**, *239*, 121704. [CrossRef]
27. Zhang, R.; Jiang, T.; Li, F.; Li, G.; Chen, H.; Li, X. Bi-level strategic bidding model for P2G facilities considering a carbon emission trading scheme-embedded LMP and wind power uncertainty. *Int. J. Electr. Power Energy Syst.* **2021**, *128*, 106740. [CrossRef]
28. He, C.; Dai, C.; Wu, L.; Liu, T. Robust Network Hardening Strategy for Enhancing Resilience of Integrated Electricity and Natural Gas Distribution Systems Against Natural Disasters. *IEEE Trans. Power Syst.* **2018**, *33*, 5787–5798. [CrossRef]